REVISTA MATÉRIA
V.25 N.02
ISSN 1517-7076 articles e-12664, 2020

The inhibitory and comparative effects of Zn-Al layered double hydroxide microcontainers intercalated with benzotriazole and nitrite for corrosion protection coatings on AISI 1010 carbon steel

Anelize Seniski [1], Rafael Frasson Monteiro[1], Gilberto Teixeira Carrera[2], Mariana d'Orey Gaivão Portella Bragança [1,3] , Kleber Franke Portella[1,3]

[1] Universidade Federal do Paraná - Politécnico/PIPE/UFPR, Avenida Coronel Francisco Heráclito dos Santos, 100, Centro Politécnico Edifício Administrativo 2º andar, CEP: 81531-980, Jardim das Américas, Curitiba, PR, Brasil.
[2] Lactec – Lame - Rodovia BR-116, km 98, nº 8.813, Jardim das Américas, CEP: 81531-980, Curitiba, Paraná, Brasil.
[3] Centrais Elétricas do Pará, Av. Augusto Montenegro, s/n - KM 8,5, CEP: 66823-010, Coqueiro, Belém, PA, Brasil.
e-mail: pipe@ufpr.br, ane.seniski@gmail.com, rafaelfrasson_monteiro@hotmail.com, gilberto.carrera@equatorialenergia.com.br, mariana.portella@lactec.org.br, portella@lactec.org.br

ABSTRACT

The electrochemical impedance spectroscopy and the open circuit potential techniques were used to analyse coatings with layered double hydroxides intercalated with benzotriazole (BTA), nitrite (NO_2), and a combination of the two. These materials were added 5% (m/m) to epoxy resin and applied on carbon steel surface as an anticorrosive system. The analyses were performed during 1000 h of salt spray chamber exposure. Morphology and particle distribution on the coatings were characterized by FEG-SEM. The LDH BTA formed a complex with zinc from the LDH layer and a phase based on ZnO/ZnOH, as shown by XRD analysis. This complex may have impaired the LDH-BTA^- corrosion inhibition process, as it formed an undesired phase on Zn-Al layers. The LDH NO_2^- enhanced corrosion resistance, inducing formation of a passivating layer on the metal surface due to corrosion inhibitor release and chloride ion capture.

Keywords: LDH, Zn-Al- NO_2^-, Zn-Al- BTA^-, Corrosion, Electrochemical impedance spectroscopy.

1. INTRODUCTION

The atmospheric corrosion of metals is an electrochemical process that starts when a thin film electrolyte layer is formed on the exposed metal. The corrosion process depends on a series of factors, such as the length of time that the surface is wet, the electrolyte pH, temperature, exposure conditions, composition of the metal, properties of the formed oxide, atmospheric pollution, etc. [1,2].

When iron or carbon steel alloys are exposed to the atmosphere, a thin layer of magnetite (Fe_3O_4) is formed, covered by a layer of FeOOH. In the presence of some pollutants, such as chloride ions, the outer layer of the passive film is displaced due to the catalytic formation of FeOCl. This compound, in the presence of high concentrations of chloride ions, dissociates and forms Fe^{3+}, resulting in more corrosion products [3].

A strategy used to control metallic corrosion is the use of barriers, such as polymeric coatings. However, during the useful life of the material, the coating mechanical properties can be altered, leading to faults that propagate and expose the substrate to the atmosphere. Consequently, the aggressive ions (such as chloride ions), water and oxygen penetrate through them, and corrosion processes starts [4,5].

An alternative to prevent the penetration of the chlorides ions and retard the corrosion process consists of incorporating layered double hydroxides (LDH) loaded with corrosion inhibitors in resin matrix coatings. The LDHs are hydrotalcite compounds and anion exchangers. Their structure consists of a metal hydroxide layered with mixed metal (M^{II}-M^{III}) positive charges separated by anions (A^{y-}) and water molecules in the interlayer. The general formula for the most common LDHs is shown in Eq. 1 [6,7,8,9]

$$[M^{II}_{1-x}\, M^{III}_{x}(OH)_2]^{x+}(A^{y-})_{x/y}.zH_2O \quad (1)$$

Autor Responsável: Anelize Seniski Data de envio: 03 /10 /2019 Data de aceite: 24/03/2020

10.1590/S1517-707620200002.1064

Several materials can be intercalated between LDH layers. The anions intercalated in the interlayer domain can be substituted for others by variation of temperature, pH, etc. These exchange properties allow intercalation of anions of different size, configuration and charge [3,4,5]. Small anions with relatively high charge density are generally the most preferable. The anions Cl^- and SO_4^{2-} are about in the middle of the anionic exchange preference series, therefore in corrosion processes the LDHs can perform similar to a trap for these aggressive ions due to these anion exchange properties [5,6,10].

The LDH intercalated with 1,2,3 benzotriazole (BTA^-) is an effective corrosion inhibitor for different metals. The BTA^- forms an effective complex with iron, when applied on its surface and its alloys, leading to formation of a protective barrier layer. The BTA^- hindered iron anodic reactions due to adsorption interaction between BTA^- and the metal surface [6,11].

Another possibility to prevent metallic corrosion is LDH intercalated with nitrite (NO_2^-). In iron or in its alloys, these ions react with ferrous ions and form an Fe_2O_3 protective layer, that behaves as anodic inhibitor, decreasing the corrosion rate. Although, when the surface is already passive, inadequate dosages of nitrite ions enhance the risk of pitting. However, with the addition of LDH intercalated with NO_2^-, these ions can be released on demand, avoiding high doses [12,13].

Xu *et al*. [13] prepared Mg-Al-LDH of nitrite and nitrate to study the absorption of chloride ions. The results showed that the LDHs intercalated with NO_2^- had better anticorrosive performance than those intercalated with NO_3^-, since the nitrite ions exert an inhibiting effect.

In the study of Zheludkevich *et al*. [14] the Mg-Al and Zn-Al-LDHs were tested, in a polymer matrix for aluminium alloy corrosion prevention. According to the authors the Zn-Al-LDH was a better corrosion inhibitor. This LDH leads to significant improvement of the corrosion protection providing an additional active protection effect [14].

Hayatdavoudi and Rahsepar [15] prepared a zinc-rich epoxy coating with Zn-Al-LDH intercalated with 2-mercaptobenzotriazole ($MBTA^-$) for corrosion protection of carbon steel. According to the authors the barrier effect of the epoxy and the inhibition action of Zn-Al-$MBTA^-$ decreased the local corrosion and enhanced the protective performance and effective lifetime of the coating [15].

In the present investigation the corrosion resistance of carbon steel 1010 plates, coated by suction airless spray gun paint system with epoxy resin incorporated with commercial LDH microcontainers intercalated with NO_2^-, BTA^- and a combination of the two was evaluated in a salt spray chamber. The protective performance provided by LDH films was characterized by electrochemical impedance spectroscopy (EIS) and by the open circuit potential (OCP). The XRD and SEM-FEG analyses were applied to characterize the LDH structure and morphology.

2. MATERIALS AND METHODS

2.1 Materials and Characterization Methods

The substrate used in this research were plates of carbon steel, which were characterized as AISI 1010 [16]. The carbon steel chemical composition, was: carbon 0.10 wt%, silicon 0.02 wt%, manganese 0.42 wt%, phosphor 0.012 wt% and sulphur 0.004 wt%. The plates were prepared in dimensions of (150 x 100 x 2) mm and the carbon steel surface was cleaned according to the international standard ISO 12944-4 1998 [17].

The coatings were developed with a clear epoxy resin (bisphenol A) and a hardener material (amine base). The LDHs used were commercially supplied. LDH Zn-Al benzotriazole (BTA^-) was supplied in powder, as well as the mixture of LDH with BTA^-/NO_2^-. The LDH with nitrite (NO_2^-), was obtained in slurry form. The LDH were add by 5% (m/m) in the epoxy resin, in a maximum concentration of 180 mg/l of inhibitors in the LDH, calculated by Eq. 1. When the LDH's are exposure to aggressive media, they exchange ions and parallel released the corrosion inhibitor so the released of the inhibitor occurs on demand [6,7,8].

The LDH morphology was characterized using an FEG SEM-EDS, TESCAN model MIRA 3 instrument. The phase content and crystal structure of the samples were analysed using a Bruker D8 ADVANCED ECO powder diffractometer (Cu Kα radiation, step 0.02º, exposition time ~ 0.1 s per step) at room temperature. The Zn-Al-NO_2^- was dried in an oven for 12 h in 80 ºC and submitted to XRD and FEG SEM-EDS analysis. The Zn-Al- BTA^- did not require prior preparation, since it was already in powder form.

2.2 Preparation of Carbon Steel and Epoxy Coatings

Four types of epoxy coatings were prepared: (i) with benzotriazole (BTA^-) LDH in powder form; (ii) with nitrite (NO_2^-) LDH in slurry form; (iii) with benzotriazole/nitrite (BTA^-/ NO_2^-) LDH in powder form; and (iv) epoxy coating without LDH. The coatings with LDH were prepared by manually dispersing 5 wt% of the LDH into component A (bisphenol A) of the epoxy resin followed by adding component B (hardener of amine resin). The mixture and homogenization proceeded at ambient temperature (22 ºC) and relative humidity of 65%.

The epoxy coatings were applied on the carbon steel surface using a suction airless spray gun with 1.8 mm nozzle. The paint system consisted of the substrate (metal), the primer and the finishing coat. Each one was approximately 40 µm thick, and the coating thick was observed using an AKSO model AK157 ultrasonic layer thickness meter (in ferrous and nonferrous bases). The first coat (prime) was developed with the addition of LDH to epoxy matrix. The second coat was applied only with the epoxy resin. In the samples without LDH, the prime and the finish coats were made with only epoxy resin. The LDHs were not added in the second coat to avoid defects in the surface of the coating.

The primer was cured at room temperature for 4 h followed by the finishing coat application, that was cured by 24 h according to the ASTM D1654 standard International (2008) [18].

The distribution of the LDHs in the coating was evaluated using an FEG SEM-EDS, TESCAN model MIRA 3 equipment. All of the samples for FEG-SEM observation were sputtered with gold to increase surface conductivity.

After 72 h a scratch longer than 7 cm was manually produced with a scalpel, in coatings with and without LDH. The scratch was deep enough to reach and expose the substrate. The mechanical scratch was made to assess the ion exchange properties of the LDHs.

2.3 Exposition and Characterization of the Systems

The samples were exposed in a salt spray chamber at 25 to 40 ºC under aqueous spray (5% NaCl) and observed at regular intervals, following the ASTM standard B117 and ASTM D1654 standard [17,18]. The plate exposure ended when the coating showed a displacement of the epoxy resin in the scratch, and that happened at approximately 1000 h.

The open circuit potential (OCP) and the electrochemical impedance spectroscopy (EIS) were used to evaluate the corrosion protection. The electrochemical analysis was performed in a cell with distilled water as electrolyte, to avoid corrosion influence of the electrolyte. A three-electrode system was used with the sample as the working electrode, with 3.14 cm² of exposed area; a saturated calomel electrode (SCE) as the reference; and a cylindrical graphite as the counter electrode (12.75 cm²). The measurements were realized in a Metrohm Autolab Potentiostat model PGSTAT 100.

The OCP and EIS tests were developed after 24, 48, 72, 100, 300, 500, 700 and 1000 h of chloride exposure. To stabilize the electrochemical cell, the samples were immersed for 50 min (approximately) before the tests. The OCP results were obtained after the system stabilization. Then, the EIS measurements were performed applying a 10 mV amplitude signal, in OCP, to a frequency range of 100 kHz to 10 mHz. These analytical conditions for EIS analysis were based on similar research [5,20,21].

The four coatings were, also, evaluated for values of their impedance modulus at the lowest frequency value ($|Z|_{1\ Hz}$ or $|Z|_{10\ mHz}$) versus the exposure time, obtained by the EIS analysis (10^{-2} Hz), according to Hang *et al*. [22].

In the end of the exposure time, before the OCP and EIS tests, the samples were photographed to register the visual analyses of the corrosion process.

3. RESULTS

3.1 Characterization of the LDHs

In the Figure 1 the XRD patterns of the BTA^- and NO_2^- LDHs are shown.

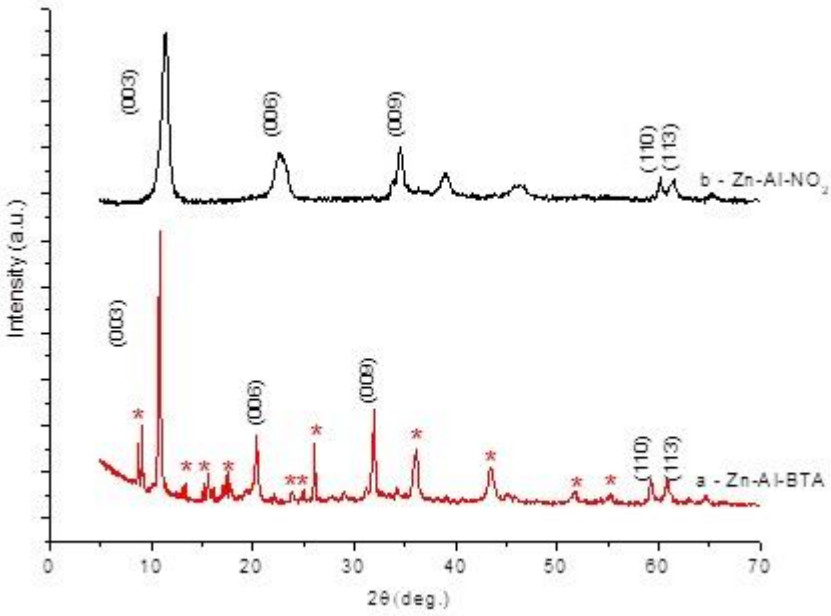

Figure 1: XRD patterns of LDH intercalated with a) Zn-Al-BTA$^-$ and b) Zn-Al-NO_2^-. The diffraction reflections with unidentified peaks are labelled with asterisks.

The SEM images of the dried Zn-Al LDH's powders are shown in Figure 2.

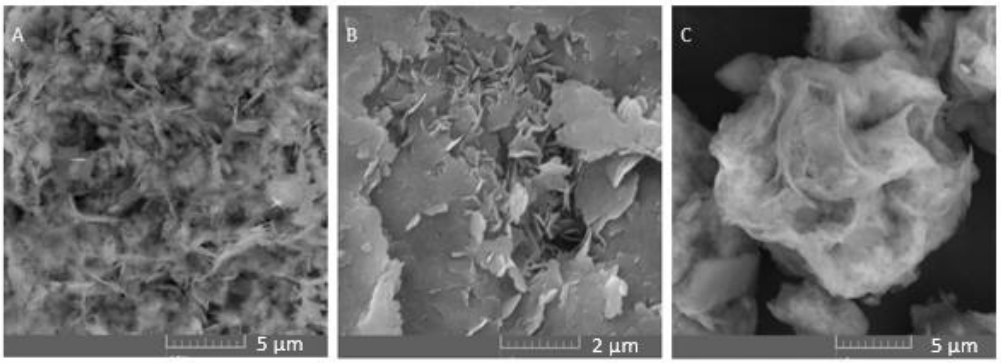

Figure 2: SEM images of LDH powders: a) Zn-Al-BTA$^-$, b) Zn-Al-NO_2^- and c) Zn-Al-BTA$^-$/NO_2^-

3.2 Characterization of the coatings

In the Figure 3 are present the Zn-Al LDH's coatings analysed by FEG-SEM.

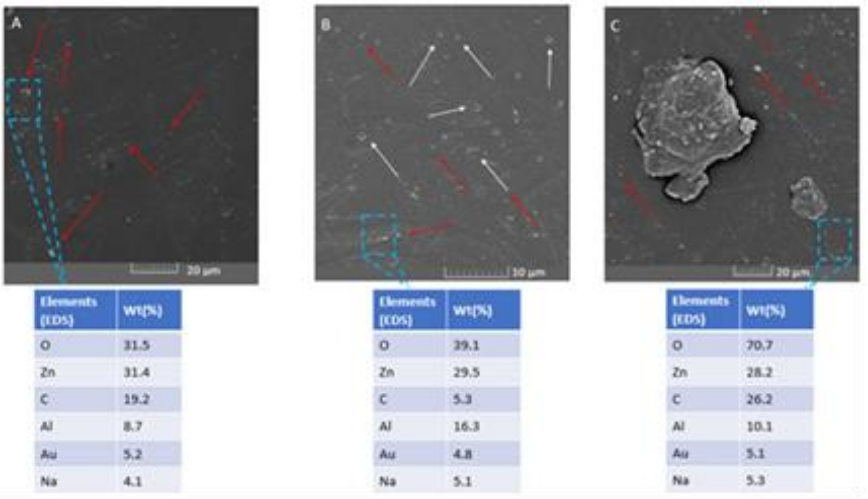

Elements (EDS)	Wt(%)
O	31.5
Zn	31.4
C	19.2
Al	8.7
Au	5.2
Na	4.1

Elements (EDS)	Wt(%)
O	39.1
Zn	29.5
C	5.3
Al	16.3
Au	4.8
Na	5.1

Elements (EDS)	Wt(%)
O	70.7
Zn	28.2
C	26.2
Al	10.1
Au	5.1
Na	5.3

Figure 3: SEM/EDS images of the epoxy resin surface with LDH's coated sample a) Zn-Al-BTA-, b) Zn-Al-NO2- and c) Zn-Al-BTA-/NO2-. The white arrows indicate the pores and the red arrow indicates the LDH distribution on the coating.

3.3 Electrochemical study

In the Figure 4 are shown the evolution of the open circuit potential (OCP) recorded before acquisition of EIS data.

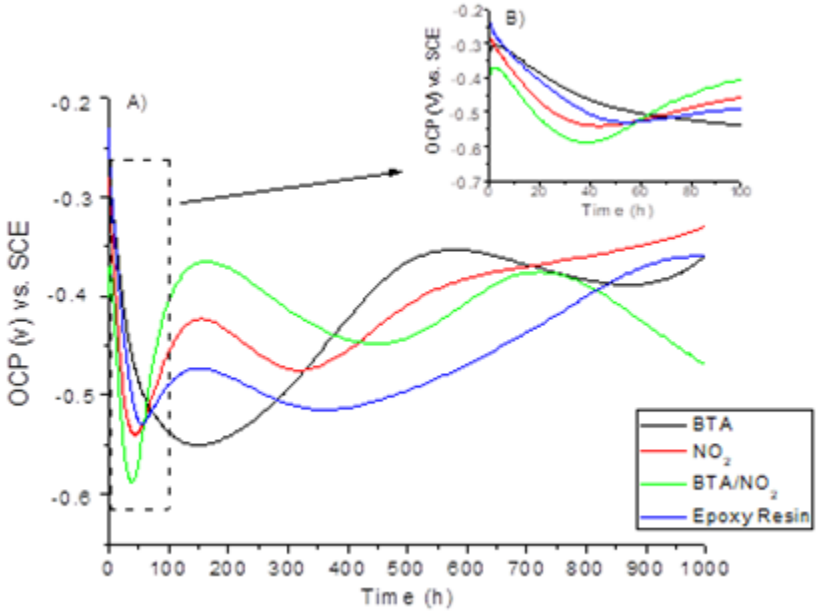

Figure 4: Evolution of the open circuit potential (OCP) recorded before acquisition of EIS spectra for the coating with LDHs Zn-Al-BTA^-, Zn-Al-NO_2^-, Zn-Al-BTA^-/NO_2^- and only epoxy resin. a) full graphic b) The detail (enlargement) of the highlighted region (0 to 100 h).

The Figure 5 shows the Bode spectra in the initial time and 100 h of exposure in salt spray chamber.

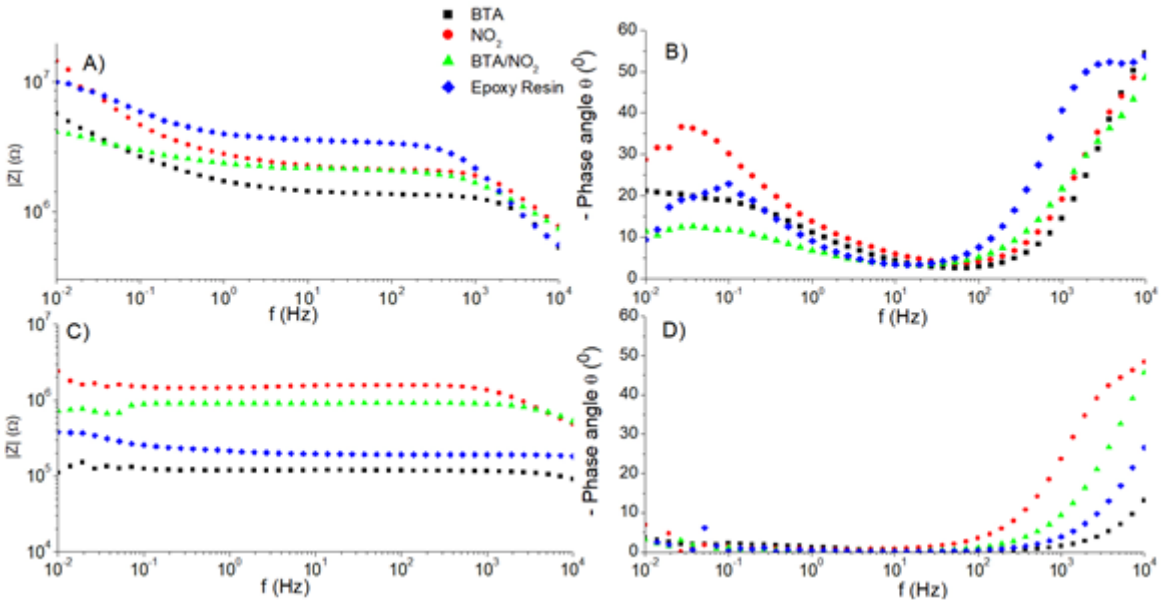

Figure 5: Bode plots of the coating with a defect and LDHs Zn-Al-BTA$^-$, Zn-Al-NO_2^-, Zn-Al-BTA$^-$/NO_2^- and only epoxy resin. (A. B) initial. (C. D) 1000 h.

Figure 6 shows the impedance value module analysis in the lower frequency range (|Z|1 Hz or |Z|10 mHz) versus exposure time.

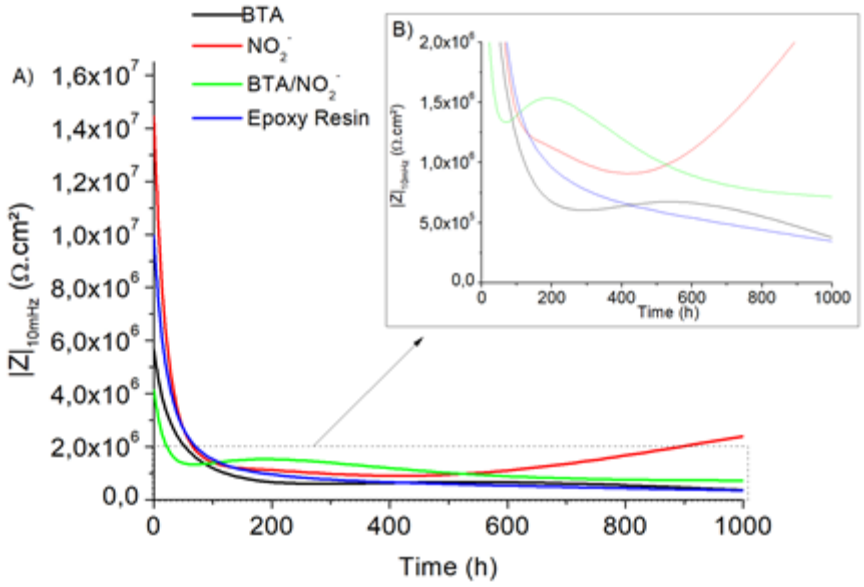

Figure 6: $|Z|_{10mHz}$ versus 1000 h of salt spray chamber exposure time for LDHs Zn-Al-BTA$^-$, Zn-Al-NO_2^-, Zn-Al-BTA$^-$/NO_2^- and only epoxy resin. a) Full graphic b) The detail (enlargement) of the highlighted region (0 to 100 h)

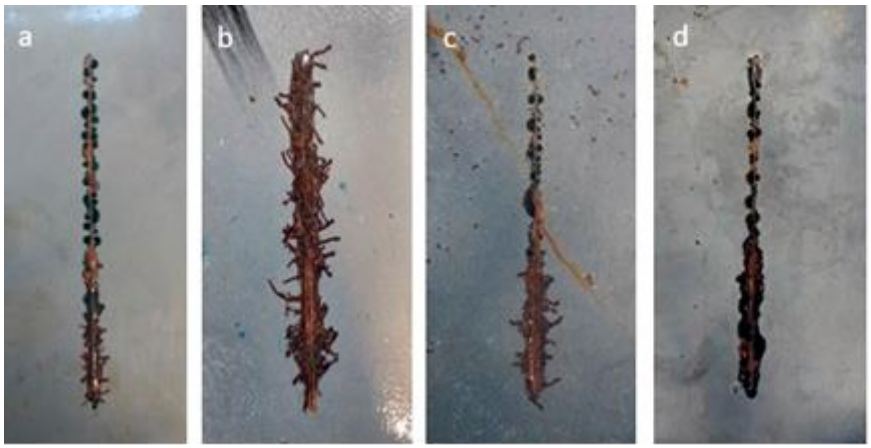

Figure 7: Optical photographs of the samples after 1000 h of exposure in salt spray chamber. a) Zn-Al-NO_2^-, b) Zn-Al-BTA^-, c) Zn-Al-BTA^-/NO_2^- and d) only epoxy resin.

4. DISCUSSION

4.1 The Characterization of the LDHs

The XRD patterns of the BTA^- and NO_2^- LDHs are shown in Figure 1. The main LDH diffraction peaks are located at NO_2^- spectra 2Θ = 11.46, 22.70, 34.32, 60.12 and 61.40 and BTA^- spectra 2Θ = 10.93, 20.36, 32.00, 59.23 and 60.85 corresponding to the (003), (006), (009), (110) and (113) planes of a layered hydrotalcite-like material, respectively. The basal spacing distance (003), calculated from peak position with the Bragg equation [23,24,25], was 0.78 nm for the LDH NO_2^- and 0.87 nm for the LDH-BTA^-. The LDH structure is seen in all the patterns, but for the LDH of NO_2^- it was verified by sharp and symmetric peaks indicating that this LDH was well crystallized [9,6].

The XRD of the Zn-Al NO_2^- (Figure 1), was similar to those presented in the literature [13,24]. However, the sample of LDH-BTA^- had other diffraction peaks (*), not identified in the XRD pattern. Serdechnova [6] suggested that zinc could form a complex with the benzotriazole and that the unidentified phases could be a product of the reaction with the LDH layer ZnOH and BTA^-. Therefore, the attempt to intercalate BTA^- into Zn-Al-LDH results in reactions with partial substitution of OH^- and partial decomposition of the parent LDH followed by formation of phases based on ZnO/ZnOH and BTA^-. The SEM images of the dried Zn-Al LDH's powders are shown in Figure 2. In it can be seen particles of "flake-shaped" (Zn-Al- NO_2^-) and "plate like" (Zn-Al- BTA^-) which is typical of LDH material [6].

4.2 Characterization of the coatings

Figure 3 presents the Zn-Al LDH's coatings analysed by FEG-SEM. The coatings consist of a uniform distribution of LDH on the epoxy resin matrix. The EDS (Figure 3) analysis shows the presence of Zn and Al indicating the LDH's. The O, C and Na may indicate the film of epoxy resin and the presence of gold were due to metallization to increase surface conductivity. The thickness of the coatings with and without LDHs was approximately 80 µm.

The coating with Zn-Al- BTA^- in Figure 3A exhibited a good distribution of the LDH particles (red arrows). The coating containing the LDH-NO_2^- in Figure 3B, had higher numbers of pores (white arrows) compared to the others, which could have been because the LDH-NO_2^- was in a slurry that may have affected epoxy resin curing due the solvents (xylene and propanol) in the mixture. These solvents evaporate and create surface pores.

Particle agglomerates were seen in the coating with Zn-Al- BTA^-/NO_2^- (Figure 3C) with average size of 20 µm. These agglomerates may have created defects on the coating surface, as commented in section 2.

4.3 Electrochemical study

Figure 4 shows the OCP results. The values variation may be associated with the kind of exposure, because the samples did not stay in electrolyte immersion. Thus, when the samples were submerged in the solution,

the formed oxides may have partially dissolved.

In the initial exposure times (up to 40 h), as shown in Figure 4b, the OCP values for the pure epoxy resin were more noble and more electronegative values were verified for samples containing LDH-NO_2^-. These initial results may be correlated with the epoxy resin adherence within the substrate. For the samples that contain only epoxy resin, there was no pore formation but in the system with LDH, therefore, the formation of pores was observed in the coating with LDH-NO_2^- and with particle agglomerations of the coating with LDH-BTA^-/ NO_2^- that created superficial pores, as shown in Figure 3A,B and C. The pore occurrence, as suggested by Tang *et al*. [26], may contribute to surface electrolyte permeation affecting the initial OCP results (Figure 4B). However, after filling the pores with electrolyte, the coating that contains LDH-NO_2^- blocked the aggressive ion permeation. Therefore, the coating obtained more noble OCP values (-0,33 V).

After 100 h of exposure (Figure 4B), for all samples, the OCP values had a tendency to diminish for more negative values. It may indicate the reductive dissolution of the oxide film formed at the metal surface. After 100 h of exposure, there was new surface oxide precipitation. The occurrence of these oxides increased the OCP values for all samples, except the sample with BTA^-, which slowly responded to this dissolution, initializing new oxide formation within 150 h. This may have occurred due the LDH-BTA^- forming phases based on ZnO/ZnOH composition, as shown on the XRD diffractogram in Figure 1.

At 1000 h of exposure, as shown in Figure 4A, the tendency of the OCP curves indicated that the samples with LDH presented more noble results than the sample with only epoxy resin. This may be correlated with pore filling due to release of corrosion inhibitor from LDHs. It is suggested that the anodic reactions of the carbon steel exposed to chlorides ions slowed the oxidation of these systems. The coatings with Zn-Al- NO_2^- presented a less negative OCP value (-0.33 V). However, only with the OCP results was not possible to decide which samples have the more resistance of corrosion at 1000h of exposure.

Figure 5 shows the Bode spectra. In the high frequency values (10^2-10^4 Hz), in the beginning of the exposition time (Figure 5A and B), all the samples presented capacitive behaviour (Figure 5B). In the Figure 5D for 1000 h of exposure, the diagram was characterized by two time constants: the first at higher frequencies, attributed to capacitive behaviour due to the epoxy film; the second was verified in lower frequencies (10^{-1} - 10^{-2} Hz) and was associated with initial electrochemical activation described for the charge transfer resistance related to the formation of the electric double layer in the artificial defect.

In the intermediate frequencies (10^{-1}-10^2 Hz), in the beginning of the exposure (Figure 5A), the coating with only epoxy resin had higher impedance (approximately $2x10^6$ Ω), representing good epoxy resin homogenization on the metal surface, with less pore formation. It was suggested that the epoxy resin film formation occurred properly, which corroborated with the OCP results. Nevertheless, with the lapsed time of chloride ion exposure, the impedance tended to decrease (to $1x10^5$ Ω at 1000 h), indicating coating degradation, corroborating the results shown in Figure 4.

Still in the exposure initial time in lower frequencies (10^{-1} - 10^{-2} Hz), in Figure 5A, the coatings with only epoxy resin and the LDH-NO_2^- presented higher impedance than the studied systems, proximally $3x10^6$ and $5x10^6$ Ω, respectively. The LDH-BTA^- and BTA^-/NO_2^- coatings exhibited impedance values of $2x10^6$ and $1x10^6$ Ω, respectively. It suggests that the impurity found on the LDH-BTA^- influenced the initial coating corrosion resistance, affecting the resin epoxy film formation, as verified on the SEM/FEG film characterization (Figure 3).

After 1000 h of the exposure to chloride ions, the impedance values (Figure 5C), for all samples, tended to reduce at least a decade in relation to the initial values (Figure 5A). In Figure 5D and in higher frequencies, all the samples demonstrated capacitive behaviour due to the coating and oxide formation on the substrate surface. Still in higher frequencies the coatings with LDH-NO_2^- exhibited higher impedance (approximately $5x10^5$ Ω). The coating with LDH-BTA^- showed values with two decades of difference ($1x10^7$ Ω decaying to $1x10^5$ Ω), compared to the exposure start time (~$6x10^4$ Ω), that exhibits lower impedance for the coating with only epoxy resin ($1x10^5$ Ω). Additionally, the BTA^-/NO_2^- mixture coating had lower impedance than the coating with NO_2^-, and higher values than the coating with BTA^- (~$3x10^5$ Ω), due the LDH-NO_2^- in the mixture.

In Figure 5D and in lower frequencies, for all samples, the phase angle decayed with decreasing frequency values, suggesting that the metal showed resistive behaviour due the oxide formation on the carbon steel surface. In the Figure 5C the impedance values for the coating with LDH-NO_2^- presented higher values through the analysed systems ($7x10^5$ Ω). In this case, it was inferred that the LDH functioned like a trap, capturing the aggressive ions and releasing the corrosion inhibitor (NO_2^-). It may have formed a passive film

that inhibited the anodic dissolution of carbon steel reaction, reducing the corrosion rate and delaying substrate degradation.

Figure 6 shows the impedance value module analysis, according to Hang *et al*. [22]. This analysis of the impedance module data in lower frequencies provides an estimate of coating corrosion protection. All samples decreased in the first hours of exposure (0-200 h), but after approximately 600 h, the impedance of the coating with LDH-$NO2^-$ increased from $9.48x10^5$ to $1.13x10^6$ Ω, suggesting ionic exchange of the LDH with the environment and release of the corrosion inhibitor. The presence of this inhibitor increased the coating resistance, protecting the metallic substrate and indicating an improvement in corrosion resistance for this system compared to the others.

Figure 7 shows the samples with the artificial defect, exposed for 1000 h in salt spray chamber. The photos of the corrosion process are in agreement with the results observed in the Bode spectra (Figure 5C and D). The results obtained using the EIS technique corroborate with the others applied, indicating the viability of LDHs, especially with intercalated nitrite, for corrosion protection in chloride ion environments.

5. CONCLUSION

Four kinds of epoxy resin coatings were prepared: adding commercial benzotriazole (BTA^-), nitrite (NO_2^-), and benzotriazole/nitrite (BTA^-/NO_2^-) LDHs, and a sample of pure epoxy resin. The LDHs were characterized in powder, by XRD and FEG-SEM. The morphology and the diffraction peaks of the LDH-NO_2^- indicate that it was well crystallized. The intercalation of the BTA^- in the Zn-Al LDHs did not perform well as shown by XRD, because of the irreversible formation of a compound based on ZnOH/ZnO and BTA^-. Good particle distribution was observed with FEG-SEM in the coatings. The results of the electrochemical techniques showed that the addition of LDHs intercalated with BTA^- did not significantly increase the corrosion resistance due to failure to intercalate the BTA^- into Zn-Al layers. Although, the LDH NO_2^- improved the epoxy coating corrosion protection for 1010 carbon steel by working like a trap for aggressive ions and releasing corrosion inhibitors.

6. ACKNOWLEDGEMENTS

This work was supported by ANEEL (PD 0371-0023/2016), CELPA/CEMAR, LACTEC, UFPR-PIPE, CNPq, CAPES and Smallmatek Lda.

7. BIBLIOGRAPHY

[1] MORCILLO, M., DE LA FUENTE, D., DÍAZ, I., *et al*., "Atmospheric corrosion of mild Steel", *Revista de Metalurgia*, Madrid, v.34, p. 35-41, 2011.

[2] LI, S., HIHARA, L.H., "The comparison of the corrosion of ultrapure iron and low-carbon steel under NaCl-electrolyte droplets", *Corrosion Science*, v.108, pp.200-2004, 2016.

[3] HIHARA, L.H. *Intelligent Coatings for Corrosion Control*, 2015.

[4] SAMADZADEH, M., BOURA, S.H., PEIKARI, M., *et al*., "A review on self-healing coatings based on micro/nanocapsules", *Progress in Organic Coatings*, v.68, pp. 159-164, 2010.

[5] TEDIM, J., KUZNETSOVA, A., SALAK, A.N., *et al*., "Zn-Al layered double hydroxides as chloride nanotraps in active protective coatings", *Corrosion Science*, v.55, p.1-4, 2012.

[6] SERDECHNOVA, M., SALAK, A.N., BARBOSA, F.S., *et al*., "Interlayer intercalation and arrangement of 2-mercaptobenzothiazolate and 1,2,3-benzotriazolate anions in layered double hydroxides: In situ X-ray diffraction study", *Journal of Solid State Chemistry*, v.233, pp. 158-165, 2016.

[7] TEDIM, J., ZHELUDKEVICH, M.L., BASTOS, A.C., *et al*., "Influence of preparation conditions of Layered Double Hydroxide conversion films on corrosion protection", *Electrochimica Acta*, v.117, pp. 164-171, 2014.

[8] FORANO, C., HIBINO, T., LEROUX, F., *et al.*, *Layered Double Hydroxides*, Chapter 13.1, 2006.

[9] ALIBAKHSHI, E., GHASEMI, E., MAHDAVIAN, M., *et al*., "A comparative study on corrosion inhibitive effect of nitrate and phosphate intercalated Zn-Al- layered double hydroxides (LDHs) nanocontainers incorporated into a hybrid silane layer and their effect on cathodic delamination of epoxy topcoat", *Corrosion Science*, v.115, p. 159-174, 2017.

[10] SALAK, A.N., TEDIM, J., KUZNETSOVA, A.I., *et al.*, "Thermal behavior of layered double hydroxide Zn-Al-pyrovanadate: Composition, structure transformations, and recovering ability", *Journal of Physical Chemistry C*., v.117, pp.4152-4157, 2013.

[11] LIU, X., CHENG, Y., WANG, W., *et al*., "Application of 1D attapulgite as reservoir with benzotriazole for corrosion protection of carbon steel", *Materials Chemistry and Physics*, v.205, pp.292-302 2018.

[12] VALCARCE, M.B., VÁZQUEZ, M., "Carbon steel passivity examined in solutions with a low degree of carbonation: The effect of chloride and nitrite ions", *Materials Chemistry and Physics*, v.115, pp.313-312 2009.

[13] XU, J., SONG, Y., TAN, Q., *et al.*, "Chloride absorption by nitrate, nitrite and aminobenzoate intercalated layered double hydroxides", *Journal of Materials Science*, v.52, pp.5908-5916, 2017.

[14] ZHELUDKEVICH, M.L., POZNYAK, S.K., RODRIGUES, L.M., *et al.*, "Active protection coatings with layered double hydroxide nanocontainers of corrosion inhibitor", *Corrosion Science*, v.52, p. 602-611 2010.

[15] HAYATDAVOUDI, H., RAHSEPAR, M. "Smart inhibition action of layered double hydroxide nanocontainers in zinc-rich epoxy coating for active corrosion protection of carbon steel substrate", *Journal of Alloys and Compounds*, v.711, pp.560-567, 2017.

[16] CLASSIFICATION OF STEELS BASE METALS CODE DESIGNATIONS AND FILLER METAL CLASSIFICATIONS AS PER AISI, SAE, ASME and CSA AISI-SAE Classification of Steels AISI-SAE Standard carbon steels, 218–228.

[17] INTERNATIONAL ORGANIZATION FOR STANDARDIZATION: ISO 12944-8, "Paints and varnishes - corrosion protection of steel structures by protective paint systems", 1998.

[18] AMERICAN SOCIETY FOR TESTING AND MATERIALS: ASTM D1654 "Evaluation of Painted or Coated Specimens Subjected to Corrosive Environment", 2008.

[19] AMERICAN SOCIETY FOR TESTING AND MATERIALS: ASTM B117, "Standard Practice for Operating Salt Spray (FOG) Apparatus", 2003.

[20] FERREIRA, M.G.S., ZHELUDKEVICH, M.L., TEDIM, J., *et al*., "Corrosion Protection and Control Using Nanomaterials", 1 ed, Woodhead Publishing Limited, 2012.

[21] LEAL, D.A., RIEGEL-VIDOTTI, I.C., FERREIRA, M.G.S., *et al*., "Smart coating based on double stimuli-responsive microcapsules containing linseed oil and benzotriazole for active corrosion protection", *Corrosion Science*, v.130, pp.56-63, 2018.

[22] HANG, T.T.X., TRUC, T.A., DUONG, N.T., *et al.*, "Layered double hydroxides as containers of inhibitors in organic coatings for corrosion protection of carbon steel", *Progress in Organic Coatings*, v.74, pp. 343-348, 2012.

[23] HU, M., YAN, X., HU, X., *et al.*, "High-capacity adsorption of benzotriazole from aqueous solution by calcined Zn-Al layered double hydroxides", *Colloids and Surfaces A*., v.540, pp.207-214, 2018.

[24] XU, J., SONG, Y., ZHAO, Y., *et al*., "Chloride removal and corrosion inhibitions of nitrate, nitrite-intercalated Mg–Al layered double hydroxides on steel in saturated calcium hydroxide solution", *Applied Clay Science*, v.163, p.2537-2548 2018.

[25] ZHANG, F., LIU, Z., ZENG, R., *et al.*, "Corrosion resistance of Mg – Al-LDH coating on magnesium alloy AZ31", *Surface & Coatings Technology*, v.258, pp.1152-1158, 2014.

[26] TANG, Y., WU, F., FANG, L., *et al.*, "A comparative study and optimization of corrosion resistance of ZnAl layered double hydroxides films intercalated with different anions on AZ31 Mg alloys", *Surface & Coatings Technology*, v.358, pp.594-603, 2019.

ORCID

Anelize Seniski https://orcid.org/0000-0001-9482-661X
Rafael Frasson Monteiro https://orcid.org/0000-0002-4595-6925
Gilberto Teixeira Carrera https://orcid.org/0000-0001-7524-7137
Mariana d'Orey Gaivão Portella Bragança https://orcid.org/0000-0002-2702-7196
Kleber Franke Portella https://orcid.org/0000-0002-0631-9990